

Second Quarterly Progress Report
NO1-DC-6-2111
**The Neurophysiological Effects of
Simulated Auditory Prosthesis
Stimulation**

J.T. Rubinstein, A.J. Matsuoka, P.J. Abbas, and C.A. Miller

Department of Otolaryngology - Head and Neck Surgery
The University of Iowa College of Medicine
Iowa City, IA 52242

May 27, 1997

Contents

1	Introduction	1
2	Summary of previous quarter's activities	1
3	Properties of the refractory EAP	2
4	Membrane noise and EAP growth	7
5	Implications for speech processors	11
6	Plans for next quarter	11

List of Figures

1	EAP from two stimuli in the cat with an interstimulus interval of 0.9 ms.	2
2	Stimulus paradigm to study recovery of EAP.	3
3	Refractory growth functions in the cat at a variety of interpulse intervals.	4
4	Simulated refractory growth functions obtained at a variety of interpulse intervals with the percent of fibers firing at saturation. The spike waveforms in the inset demonstrate the decreased spike amplitude during the refractory period.	5
5	Normalized refractory growth functions from the same data shown in Figure 3.	5
6	Compound RS as a function of interpulse interval. Data is obtained from the normalized refractory growth functions of 4 cats. One animal has responses recorded to both cathodic and anodic stimulation.	6
7	Input-output functions for a model node of Ranvier during the relative refractory period. Simulated on the Cray C90 at the San Diego Supercomputer Center.	7
8	Verveen's definition of threshold and relative spread (RS). For details, see text and [5].	8
9	RS of a relative refractory node of Ranvier as a function of IPI. RS calculated from the I/O functions in Figure 7.	9
10	Axon model simulations of PST histograms for a single stimulus near threshold and the second of two stimuli where the first stimulus is at a firing efficiency of 100% and the second is near threshold. IPI is 1.1 ms. Jitter is increased during the relative refractory period. Unmasked jitter is 29 μs , masked jitter is 56 μs	10
11	The relationship between single fiber RS and compound RS. When a compound RS is calculated from a population of fibers with a twofold range of threshold and an RS of .04, $RS_c = .29$. If the single fiber RS is increased to .4, $RS_c = .49$. Thus RS_c is relatively insensitive to RS	10

1 Introduction

Despite the substantial successes that have been demonstrated with cochlear implants, there clearly are limitations in the transfer of information to the central nervous system in individuals using these devices. We suggest that at least some of these limitations are related to spatial and temporal interactions occurring at the auditory nerve with all current designs of implanted prostheses. The project's research program is aimed toward the eventual development of alternative means of stimulating the auditory nerve. Our approach is to use computer simulations and experimental data to:

1. Characterize the fundamental spatial and temporal properties of intracochlear stimulation of the auditory nerve.
2. Evaluate the use of novel stimuli and electrode arrays.
3. Evaluate proposed enhancements in animals with a partially degenerated auditory nerve.

2 Summary of previous quarter's activities

- We have continued to improve our ability to hold single units by increasing the mechanical isolation of our experimental chamber. A substantial number of unit responses have been recorded.
- We are developing software for a new data acquisition board that will allow analysis of growth functions for EAP and input-output functions for single units during the experiment.
- We have obtained single unit and EAP data from 3 cats and EAP data from 3 guinea pigs.
- Dr. Loeb spent two days in our laboratory as a consultant and we performed preliminary studies using the proprietary electrode array designed to decrease spatial interactions.
- We have performed extensive analysis of EAP growth functions during the refractory period. Model simulations of these functions have also been performed.
- Our research group had three podium presentations at the midwinter meeting of the Association for Research in Otolaryngology. One

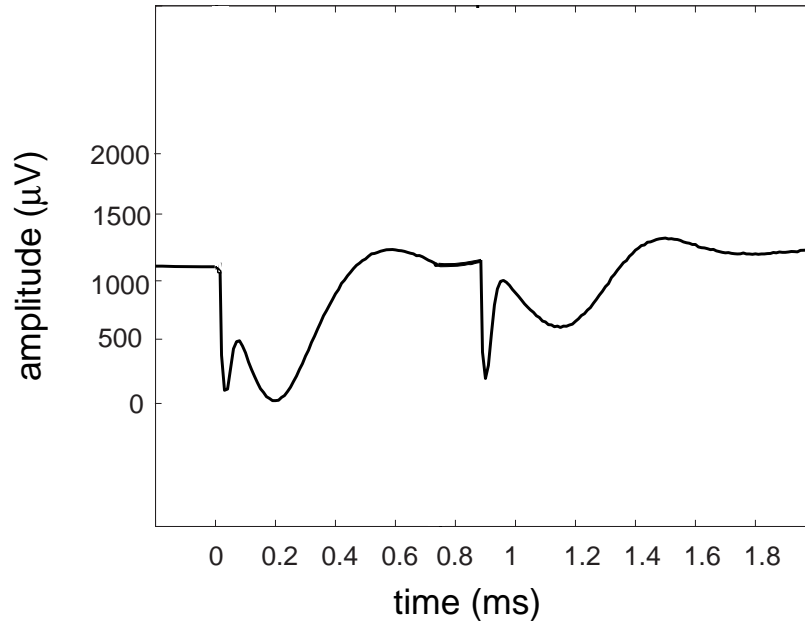


Figure 1: EAP from two stimuli in the cat with an interstimulus interval of 0.9 ms.

of these presentations was based on material from the last quarterly progress report, two on materials from this report.

3 Properties of the refractory EAP

Figure 1 demonstrates the direct nerve EAP in response to two stimuli with an interstimulus interval of 0.9 ms. It is clear that the second EAP is of significantly smaller amplitude than the first. Recovery functions as described by Brown & Abbas[1, 2] have been used to characterize the recovery process.

To allow better comparison with single unit recordings and model simulations we have used an alternate form of analysis. First a growth function is obtained for a single stimulus. Then using a masking stimulus which is of sufficient amplitude to reach saturation of the growth function, a family of growth functions for a probe stimulus are obtained at varying interstimulus intervals. Figure 2 illustrates the stimulus paradigm used in these studies.

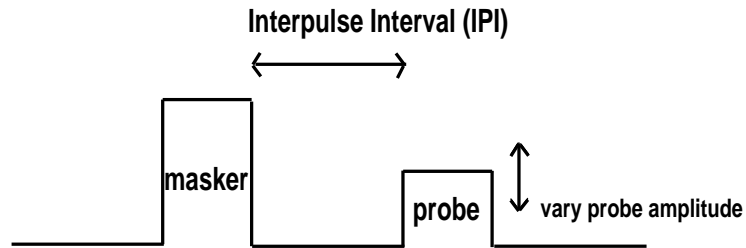


Figure 2: Stimulus paradigm to study recovery of EAP.

There are two reasons for this approach:

1. The masking pulse is presumably activating all of the stimuable spiral ganglion cells as it is of sufficient amplitude to reach saturation of a single-pulse growth function. Thus the probe pulse affects a population of “uniformly” refractory neurons. No neurons should be present that are not in the relative refractory period.
2. By analyzing growth functions during the refractory period rather than recovery functions, we can compare the EAP results with single unit and simulated input-output functions. This allows use of similar analysis tools and facilitates determination of the relative contribution of population and stochastic characteristics of refractory single fibers to the recovery of the EAP.

Figure 3 demonstrates a family of EAP growth functions obtained at different interpulse intervals (IPI). We call these refractory growth functions (RGF). It is clear that the RGFs saturate at lower amplitudes as IPI decreases. This could be due to a decrease in the population of activated neurons, as some may be absolutely refractory, or a decrease in the spike amplitude of the fibers contributing to the EAP.

We have used our computational model in an attempt to dissect out the relative contributions of these two effects on the refractory growth functions. Figure 4 demonstrates a family of RGFs as computed by the model. It also shows a decreasing saturated value of the RGF as IPI is shortened. By calculating the firing efficiency, the percentage of fibers firing, one can see

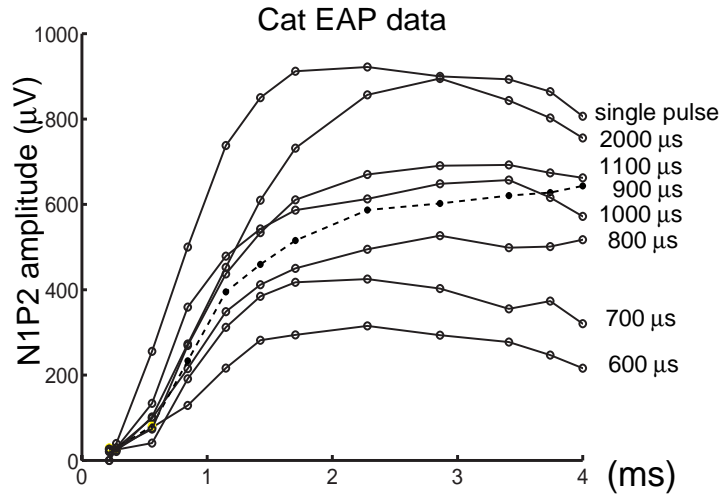


Figure 3: Refractory growth functions in the cat at a variety of inter-pulse intervals.

that as IPI decreases, initially the spike amplitude of each fiber is decreasing but all fibers are still responding. At shorter IPIs, some fibers become absolutely refractory and the firing efficiency drops below 100%. This causes a further decrement of the saturating value.

As was demonstrated in the First Quarterly Progress Report, the EAP growth function is produced by a summation of the single unit input-output functions of the fiber population contributing to the EAP. Thus we would expect the slope of the growth functions to be determined partly by the slopes of the contributing I/O functions and partly by the distribution of the single unit thresholds. To compare growth functions within and across animals and with I/O functions we normalize the growth functions to the saturating values. Each point on the growth function is then at some “% saturated” which should correlate roughly with the fraction of total fibers stimuable at maximum current levels. Figure 5 demonstrates the normalized RGFs from the same animal whose RGFs appear in Figure 3.

It is clear that the slope of the normalized RGF is dependent on the IPI in this animal with a significant decrease at an IPI of 0.9 ms. To better quantify this slope and relate it to the I/O function slope, we fit the normalized RGF

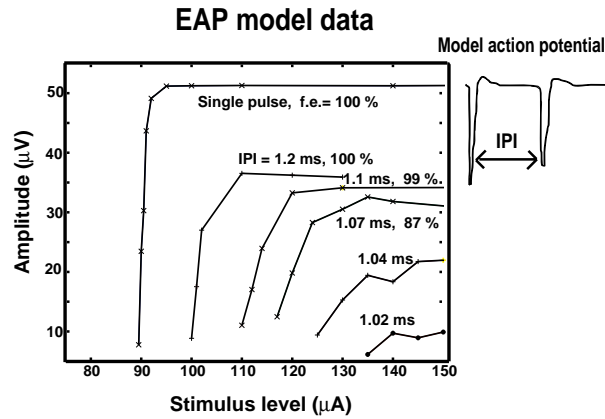


Figure 4: Simulated refractory growth functions obtained at a variety of interpulse intervals with the percent of fibers firing at saturation. The spike waveforms in the inset demonstrate the decreased spike amplitude during the refractory period.

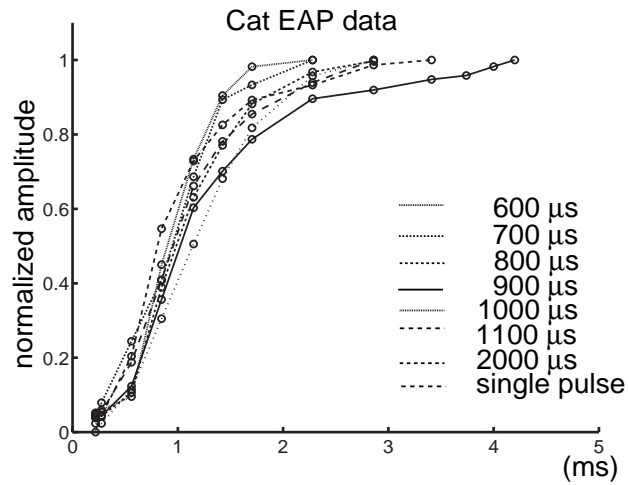


Figure 5: Normalized refractory growth functions from the same data shown in Figure 3.

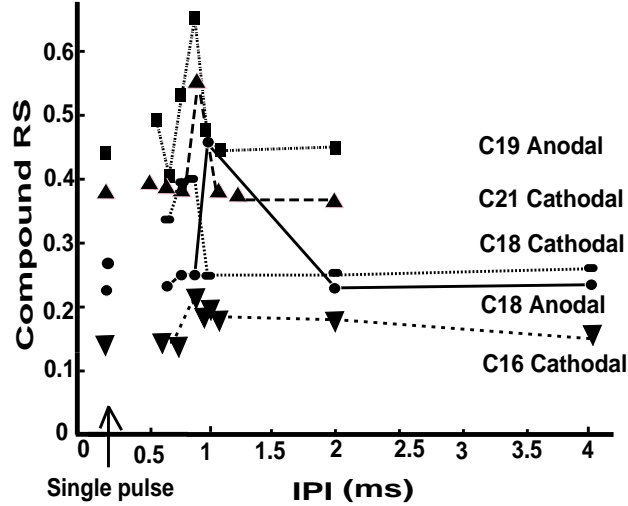


Figure 6: Compound RS as a function of interpulse interval. Data is obtained from the normalized refractory growth functions of 4 cats. One animal has responses recorded to both cathodic and anodic stimulation.

to an integrated Gaussian. The *compound threshold*, Th_c , is then defined as the stimulus current resulting in a response amplitude 50% of the saturation amplitude. The *compound RS*, RS_c , is defined as the coefficient of variation of the integrated Gaussian fit to the normalized RGF:

$$RS_c = \frac{\sigma_c}{Th_c}$$

where σ_c is the standard deviation of the integrated Gaussian. Thus our growth function definitions are consistent with the single unit I/O function definitions of threshold and RS of Verveen[5] (see Figure 8).

A plot of RS_c as a function of IPI for five recordings in four cats appears in Figure 6. It demonstrates that there appears to be a specific IPI of about 0.9 ms where RS_c increases by about a factor of two. This produces a shallower normalized RGF at this IPI relative to longer or shorter IPIs. Understanding the mechanism of this phenomenon requires a digression into single fiber membrane noise and its contribution to the EAP.

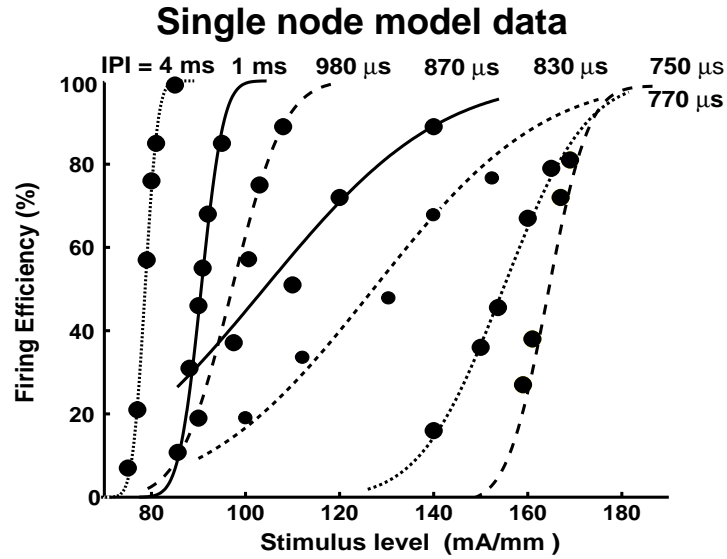


Figure 7: Input-output functions for a model node of Ranvier during the relative refractory period. Simulated on the Cray C90 at the San Diego Supercomputer Center.

4 Membrane noise and EAP growth

Using our stochastic computational model of the node of Ranvier[4] modified for mammalian sodium channel kinetics, we can plot a series of refractory input-output functions using the same stimulus paradigm as in Figure 2. These are shown in Figure 7 and they demonstrate a profound effect of IPI on the slope of the I/O function for a single node. The expected refractory effects on threshold can also be seen in the rightward shift of the functions at short IPIs.

To study the slope of the model's I/O function, the functions are fitted to integrated Gaussians and threshold and RS is calculated as per Verveen[5] (see Figure 8)

$$RS = \frac{\sigma}{Th}$$

where Th is the stimulus current at a 50% firing efficiency and σ is the standard deviation of the integrated Gaussian fit to the I/O function.

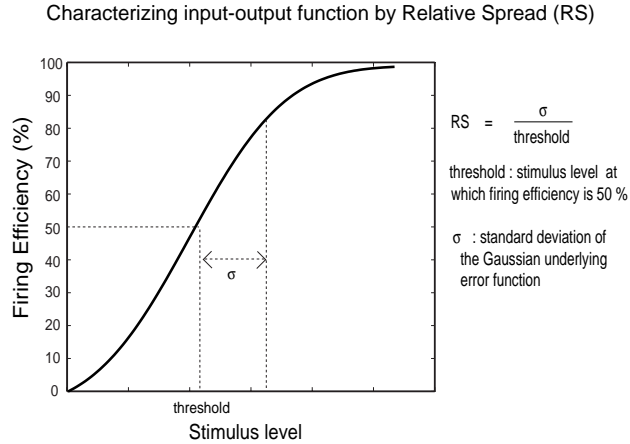


Figure 8: Verveen's definition of threshold and relative spread (RS). For details, see text and [5].

Figure 9 demonstrates the RS as a function of IPI for the I/O functions shown in Figure 7. It shows an order of magnitude increase in the RS at particular IPIs during the relative refractory period. As RS is a measure of membrane noise, this implies a dramatic increase in membrane noise during the relative refractory period at a similar IPI as observed in the cat. This occurs due to the mathematical properties of threshold and ionic channel fluctuations. Channel fluctuations are finite, threshold becomes infinite at the absolute refractory period. RS is the standard deviation of the channel fluctuations normalized by the threshold. Thus during the relative refractory period, the channel fluctuations increase due to the smaller number of sodium channels available. Threshold increases as well, but not as rapidly. When the IPI approaches the absolute refractory period, threshold diverges toward infinity and the RS decreases.

The increased membrane noise during the relative refractory period is illustrated in a different manner in Figure 10. This illustrates a post stimulus time (PST) histogram of our full axon model for a single stimulus near threshold, and for the second of two stimuli when the second stimulus is near threshold. In the two stimulus case, the first stimulus is of sufficient magnitude to evoke a firing efficiency of 100%. This shows that spike jitter, even when accounting for threshold changes, is also increased during the

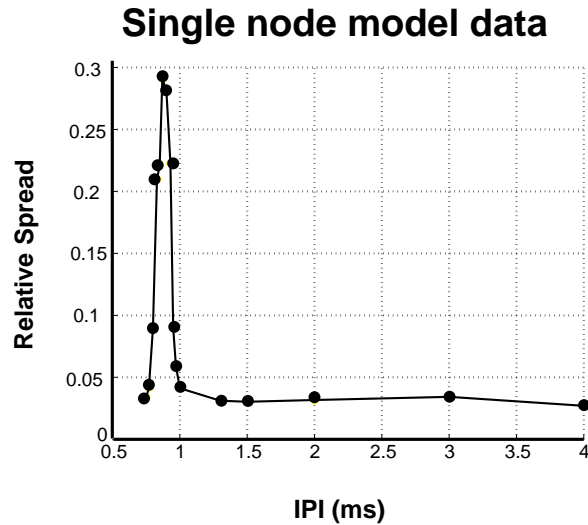


Figure 9: RS of a relative refractory node of Ranvier as a function of IPI. RS calculated from the I/O functions in Figure 7.

relative refractory period.

Jitter is a measure of noise in excitation and conduction, RS is a measure of noise of excitation. The two measures are complementary and help to localize sources of noise in both models and experimental recordings. Detailed studies are planned to quantify this phenomenon at the single unit level, but it is already clear from the EAP data in Figure 6 that the phenomenon must be occurring. However the model suggests an order of magnitude increase in single fiber RS while the EAP data shows at best a twofold increase in compound RS. This discrepancy can be readily explained by the fact that RS_c is relatively insensitive to changes in single fiber RS due to the distribution of fiber thresholds which has a far greater effect on RS_c . Figure 11 demonstrates the compound RS resulting from a population of fibers with a twofold range of thresholds and a single fiber RS of .04 (consistent with our single-unit recordings – see next progress report). If the single fiber RS is increased by an order of magnitude, the RS_c increases not quite twofold. Thus our refractory EAP data is consistent with a substantial increase in membrane noise during the relative refractory period.

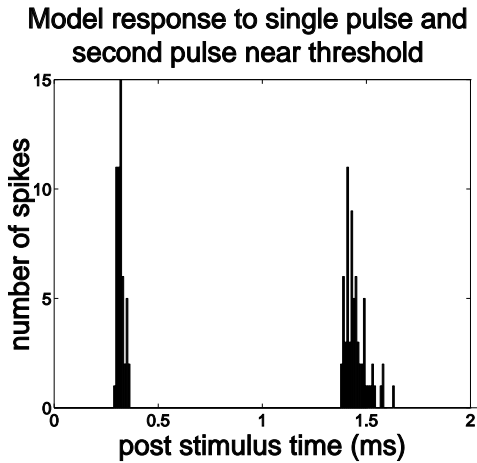


Figure 10: Axon model simulations of PST histograms for a single stimulus near threshold and the second of two stimuli where the first stimulus is at a firing efficiency of 100% and the second is near threshold. IPI is 1.1 ms. Jitter is increased during the relative refractory period. Unmasked jitter is $29 \mu s$, masked jitter is $56 \mu s$.

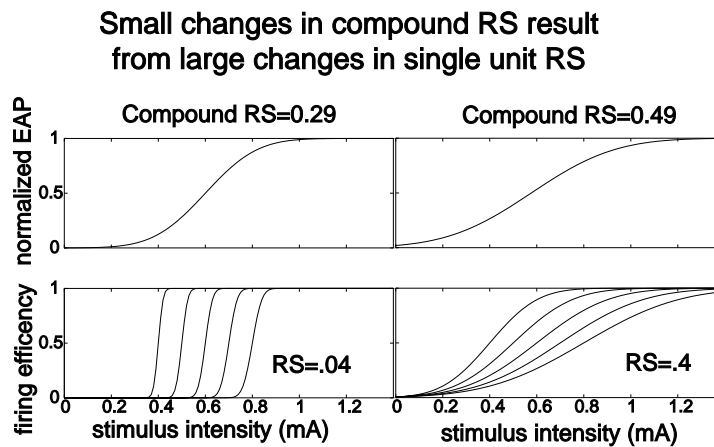


Figure 11: The relationship between single fiber RS and compound RS. When a compound RS is calculated from a population of fibers with a twofold range of threshold and an RS of .04, $RS_c = .29$. If the single fiber RS is increased to .4, $RS_c = .49$. Thus RS_c is relatively insensitive to RS .

5 Implications for speech processors

One of the significant differences between acoustic and electrical hearing is the extreme fiber synchrony imposed by electrical stimulation. This may be contrasted with acoustic stimulation where synaptic noise imparts much greater within-fiber and across-fiber noise. PST histograms in response to clicks have much greater jitter than those obtained in response to shocks. It can be demonstrated that specific amounts of independent across-fiber noise is extremely useful in representing temporal details of a stimulus. Such “stochastic resonance” is common in other sensory systems[3]. We hypothesize that part of the success of high-rate stimulation may be due to a more natural distribution of spike timing across the auditory nerve as jitter increases and synchrony decreases during stimulation at rates approaching 1000 pps (1 ms IPI).

It is currently unknown whether the human auditory nerve has the same critical IPI as the cat. Using Ineraid subjects, or subjects implanted with the new Nucleus CI24-M, we should be able to determine this IPI although the specifics of this measurement will not be as straightforward as in the cat. In addition, we will measure the critical IPI in guinea pigs to see if it generalizes across mammalian species. Ineraid subjects with CIS processors could also be studied to determine the effect of single-channel pulse rate on speech recognition.

6 Plans for next quarter

Multiple activities are planned for the current quarter. These include:

- Complete analysis of single fiber responses to single stimuli. We plan to have characterized RS and jitter for anodal and cathodal stimulation for a substantial number of fibers.
- Further software development for our new data acquisition board which will allow studies of single fibers during the relative refractory period.
- Study compound RS in the guinea pig and determine if it increases at the same IPI as in the cat.
- Characterize EAP responses to modulated pulse trains in both cat and guinea pig.

- Begin measures of channel interaction using multielectrode arrays.
- Dr. Loeb will be visiting again and we plan to conduct further experiments with the proprietary electrode design.
- Blake Wilson will be making a consulting visit.
- At least two papers will be prepared for publication based on the material in the last two progress reports.

References

- [1] Brown C.J., & Abbas P.J. (1990). Electrically evoked whole-nerve action potentials: Parametric data from the cat. *J. Acoust. Soc. Am.*, 88, 2205–2210.
- [2] Brown C.J., Abbas P.J., & Gantz B. (1990). Electrically evoked whole-nerve action potentials: Data from human cochlear implant users. *J. Acoust. Soc. Am.*, 88, 1385–1391.
- [3] Collins, J.J., Chow, C.C. and Imhoff, T.T. (1995). Stochastic Resonance Without Tuning. *Nature*, 376, 236–238
- [4] Rubinstein J.T. (1995). Threshold fluctuations in an N Sodium Channel Model of the Node of Ranvier. *Biophysical J.*, 68, 779–785.
- [5] Verveen, A.A., *Fluctuation in Excitability*, Drukkerij Holland N.V., Amsterdam, 1961.